Control of autoionization widths: Doubly excited coherent elliptic states

Daniel Janby and Lars Bojer Madsen*
Department of Physics and Astronomy, University of Aarhus, 8000 Aarhus C, Denmark

Valentin N. Ostrovsky†
V. Fock Institute of Physics, St. Petersburg State University, St. Petersburg 198504, Russia
(Received 24 January 2006; published 8 June 2006)

Doubly excited coherent elliptic states (DECESs) of an atom could be produced by exciting an atomic electron to a Rydberg state, applying the adiabatic field-switching technique to obtain a coherent elliptic state (CES) and by subsequent excitation of an atomic core electron into a low-lying excited state. The DECESs decay by autoionization and radiative transitions. As an example, the autoionization widths are calculated for DECESs in He. The dependence of the widths on the eccentricity of the CES, principal quantum number of the Rydberg electron, orientation of the inner electron orbital and electron exchange is studied and interpreted.

DOI: 10.1103/PhysRevA.73.062708 PACS number(s): 32.80.Dz, 32.80.Hd, 32.60.+i, 32.30−r

I. INTRODUCTION

The phenomenon of autoionization from multiply excited states in atomic and molecular physics has been considered in an immense number of publications since the pioneering experimental [1] and theoretical works [2]. Recently, for example, the generic cases of doubly excited states in helium [3] and triply excited states in lithium [4] were reviewed. For both doubly and triply excited states, the correlated motion of the electrons may be analyzed and characterized to some degree by collective modes of motion and associated approximate quantum numbers.

Normally the spectrum of autoionization widths presents a discrete set. Theoretically, this follows immediately from the fact that the resonance states correspond to the complex-valued poles of the S-matrix or the Green function describing the system. The spectrum has been analyzed in detail and regularities in the behavior of the widths as, e.g., one of the electrons is excited through a Rydberg series are well understood by participator and/or spectator models [5,6].

One of the current trends in atomic and molecular physics is to engineer and manipulate small quantum systems in order to obtain control of the dynamics. We therefore think it is timely also to raise such questions with respect to the autoionization dynamics. In this work we point out the possibility to vary the autoionization widths smoothly and to control them. This particular situation appears in the case of autoionizing Rydberg states where the highly excited (outer) electron, to an accurate approximation, moves in a pure Coulomb field of the residual atomic core. Then the well-known degeneracy of energy levels in the orbital quantum number ℓ of the Rydberg electron allows a smooth variation of the eigenstate of the outer electron. The degeneracy is n^2-fold (without account for the electron spin) in the pure Coulomb potential where n is the principal quantum number of the outer electron. The eigenstates may be constructed as linear combinations of basis states (the latter could be, for instance, the conventional spherical states with quantum numbers $n\ell m_\ell$). Hence the number of complex-valued parameters defining an eigenstate is (n^2-1). While the eigenstates are degenerate in energy, they can have drastically different autoionization widths. The reason is related to the fact that for the spherical states $n\ell m_\ell$ of the Rydberg electron the autoionization widths are known to decrease exponentially with the orbital quantum number ℓ [7]. Therefore the weight of different ℓ states in the linear combination plays a crucial role. In this work we address this role in detail. We introduce a new set of states, namely the doubly excited coherent elliptic states (DECESs) and study the dependence of the autoionization dynamics on the controlled motion of the coherent elliptic Rydberg state and the relative orientation between the orbit of the outer electron and the inner one. We note that more than 15 years ago circular (maximum ℓ) doubly excited states of barium were produced experimentally and found to have a very long lifetime against autoionization [8] in agreement with theoretical predictions.

The paper is organized as follows. In Sec. II, we recall the special eigenstates of the Coulomb problem known as *coherent elliptic states* (CESs) and we discuss their particular physical interest and importance. In particular, they have an appealing physical meaning being quantum analogues of classical electron elliptic orbits. In Sec. II, we also briefly describe how these states can be prepared experimentally. It is possible to address the entire range of the eccentricity parameter ε and hence to control the ℓ composition of the CES. In Sec. III, we introduce the two-electron doubly excited CESs and mention their possible extension to triply and multiply excited CESs. In that section, we also develop a scheme to calculate the autoionization widths of the DECES. The numerical results obtained in Sec. IV allow an appealing qualitative interpretation. In Sec. V, we address the question of the effects of coherence and electron-electron interactions and finally, in Sec. VI we conclude. We use atomic units ($\hbar=m_e=a_0=e=1$) throughout.

II. COHERENT ELLIPTIC STATES OF RYDBERG ATOMS

It is well known that many properties of highly excited Rydberg states can be interpreted in classical terms. It is in

*Electronic address: bojer@phys.au.dk
†Electronic address: valentin.ostrovsky@pobox.spbu.ru

this sense that the Rydberg atom forms a bridge between classical physics and quantum mechanics. In classical mechanics an elliptic electron orbit is fixed by the following parameters: (i) a unit vector $\hat{\vec{n}}_\ell$ defines the orbit plane; this vector is directed along the electron orbital momentum vector $\vec{\ell}$; (ii) fixing orientation of the orbit perihelium requires another unit vector $\hat{\vec{n}}_a$; this vector is directed along the Runge-Lenz vector $\vec{a}$ of the electron,

$$\vec{\ell} = \vec{r} \times \vec{p},$$

$$\vec{a} = n(\vec{p} \times \vec{l} - \vec{r}/r), \quad n = 1/(Z\sqrt{2|E|}),$$

$$\vec{\ell} \cdot \vec{a} = 0; \tag{1}$$

(iii) the orbit shape is governed by the absolute value of the orbital momentum ℓ, related to the eccentricity of the orbit

$$\varepsilon = \sqrt{1 - 2|E|\ell^2/Z^2}. \tag{2}$$

Here Z is the charge of the atomic nucleus. Since the eccentricity is confined to the interval $0 \le \varepsilon \le 1$, it can be conveniently parametrized in terms of the effective angle α,

$$\varepsilon = \sin \alpha. \tag{3}$$

Then the simple and useful relations are

$$\ell = n \cos \alpha, \quad a = n \sin \alpha, \quad \ell^2 + a^2 = n^2. \tag{4}$$

[the quantum counterpart of the latter formula, $\ell^2 + a^2 = n^2 - 1$, is valid also for small n $(n \sim 1)$].

Physically, fixing $\hat{\vec{n}}_\ell$ and $\hat{\vec{n}}_a$ is achieved by imposing magnetic $\vec{B}$ and electric $\vec{F}$ fields on a Rydberg atom (it is presumed that the fields are so weak that orbit distortions corresponding to the nonperturbative regime are avoided). Thus the road to the construction of quantum states similar to classical orbits goes via the consideration of the so-called linear Stark-Zeeman effect, i.e., via the study of the behavior of the hydrogen atom under the combined action of external electric and magnetic fields. This fundamental problem was treated in the old quantum mechanics, before the wave mechanics of Schrödinger, by Born [9], and in modern quantum theory by Demkov *et al.* [10]. The eigenvalues and eigenstates of the Hamiltonian were obtained for an arbitrary principal quantum number n. The semiclassical properties of these states in case of $n \gg 1$ were subsequently analyzed [11] and the relation to classical mechanics was revealed. The formula for the linear Stark-Zeeman eigenenergies

$$E_{nm_1m_2} = -\frac{Z^2}{2n^2} + \omega_1 m_1 + \omega_2 m_2, \tag{5}$$

contains quantum numbers m_1 and m_2 that run independently with units steps from $-j$ to j, $j = \frac{1}{2}(n-1)$,

$$\vec{\omega}_I = \vec{\omega}_S + \vec{\omega}_S, \quad \vec{\omega}_2 = \vec{\omega}_L - \vec{\omega}_S, \tag{6}$$

$$\vec{\omega}_S = -\tfrac{3}{2} n\vec{F}, \quad \vec{\omega}_L = \tfrac{1}{2} n\vec{B}. \tag{7}$$

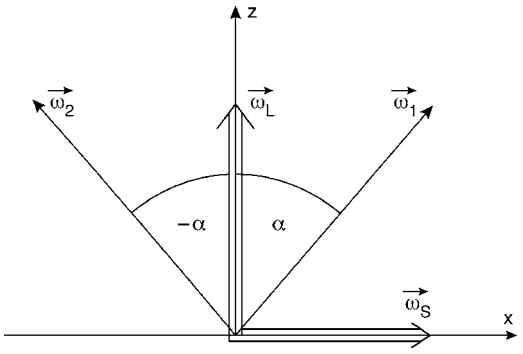

FIG. 1. Quantization directions of the external fields used in the construction of CESs.

Below we specialize to the case of perpendicular fields $\vec{F} \perp \vec{B}$ (see Fig. 1), since this configuration corresponds to the classical condition $\vec{\ell} \cdot \vec{a} = 0$. In this setup, we obtain $\omega_1 = \omega_2 \equiv \omega$ and

$$E = -\frac{Z^2}{2n^2} + \omega(m_1 + m_2). \tag{8}$$

The solution of the Stark-Zeeman problem proceeds via the construction of two *pseudospin operators*,

$$\vec{j}_1 = \tfrac{1}{2}(\vec{\ell} + \vec{a}), \quad \vec{j}_2 = \tfrac{1}{2}(\vec{\ell} - \vec{a}). \tag{9}$$

These vector operators have algebraic properties identical to the quantum angular momentum operators. They are independent, i.e., commute, $[\vec{j}_1, \vec{j}_2] = 0$, and have equal lengths: $\vec{j}_1^2 = \vec{j}_2^2 = j(j+1)$. Therefore each of them could be quantized along an independent quantization axis. The eigenstates $|nm_1m_2; \hat{\vec{u}}_1, \hat{\vec{u}}_2\rangle$ for the Stark-Zeeman problem correspond to quantization of $\vec{j}_1$ along the $\hat{\vec{u}}_1$ axis and $\vec{j}_2$ along the $\hat{\vec{u}}_2$ axis, where $\hat{\vec{u}}_1 = \vec{\omega}_1/\omega_1$ and $\hat{\vec{u}}_1 = \vec{\omega}_2/\omega_2$ are unit vectors. This is described by the relations

$$\vec{j}_1 \cdot \hat{\vec{u}}_1 |nm_1m_2; \hat{\vec{u}}_1, \hat{\vec{u}}_2\rangle = m_1 |nm_1m_2; \hat{\vec{u}}_1, \hat{\vec{u}}_2\rangle,$$

$$\vec{j}_2 \cdot \hat{\vec{u}}_2 |nm_1m_2; \hat{\vec{u}}_1, \hat{\vec{u}}_2\rangle = m_2 |nm_1m_2; \hat{\vec{u}}_1, \hat{\vec{u}}_2\rangle, \tag{10}$$

where the dependence on the unit vectors $\hat{\vec{u}}_1$, $\hat{\vec{u}}_2$ is parametric. The explicit formulas for the states $|nm_1m_2; \hat{\vec{u}}_1, \hat{\vec{u}}_2\rangle$ in terms of spherical basis $|n\ell m_\ell\rangle$ are constructed by applying finite rotation operators to the conventional parabolic, or, alternatively, spherical electron states. These expansions are well known [10,11] and will not be reiterated here. We only mention the deep group-theoretical background of the scheme. The parametric dependence on the relative fields strength is implicit in Eq. (10).

The angular momentum states with maximum modulus of projection along the quantization axis $(m = \pm j)$ are distinguished by the fact that they are minimum uncertainty states in the sense that the Heisenberg uncertainty relation is satisfied as an equality. Such states are called *coherent* states [12]. For our two-pseudospin basis of Eq. (10) we are interested mostly in the states where both projections attain maxi-

mum values of the quantum numbers m_1 and m_2: $m_1=m_2=j$. We denote this state by $|n\alpha\rangle$,

$$|n\alpha\rangle \equiv |njj;\hat{\vec{u}}_1,\hat{\vec{u}}_2\rangle. \tag{11}$$

Since these eigenstates satisfy the minimum quantum fluctuation condition, they are quantum (semiclassical) analogues of classical elliptic orbits. This justifies the name *coherent elliptic states* (CESs) for the states $|n\alpha\rangle$ [11].

For the quantitative analysis it is convenient to consider the expansion of $|n\alpha\rangle$ in the spherical basis

$$|n\alpha\rangle = \sum_{\ell m_\ell} c^{\alpha}_{n\ell m_\ell} |n\,\ell\,m_\ell\rangle. \tag{12}$$

The explicit expression for the expansion coefficients is well known [11]

$$c^{\alpha}_{n\ell m_\ell} = (-1)^{\frac{\ell-m_\ell}{2}} \frac{2^{n-\ell-1}(n-1)!}{\left(\frac{\ell-m_\ell}{2}\right)!\left(\frac{\ell+m_\ell}{2}\right)!} \times \sqrt{\frac{(\ell+m_\ell)!\,(\ell-m_\ell)!\,(2\ell+1)}{(n-\ell-1)!\,(n+\ell)!}} \times \left(\sin\frac{\alpha}{2}\right)^{n-m_\ell-1}\left(\cos\frac{\alpha}{2}\right)^{n+m_\ell-1}. \tag{13}$$

Here $\ell+m_\ell$ is even; the spherical states $|n\,\ell\,m_\ell\rangle$ are quantized along the direction of the magnetic field $\vec{B}$. The effective angle is simply expressed via electric and magnetic field strengths,

$$\tan\alpha = \omega_S/\omega_L. \tag{14}$$

Limiting cases of CESs are the circular states ($\alpha=0$, $\ell=m_\ell=n-1$) and the uppermost Stark states ($\alpha=\frac{1}{2}\pi$).

We now turn to a brief discussion of the formation of coherent elliptic states by the adiabatic field-switching method suggested by Delande and Gay [11,13,14]: First a Rydberg atom is placed into an electric field and the outermost Stark state is selectively populated by a laser excitation. Second, after this transfer of population, the magnetic field is switched on. In the case of a slow (adiabatic) switching no state-to-state transitions occur between the adiabatic states; the outermost state is correlated to the elliptic state with the effective angle α defined by Eq. (14). Thus all the initial population is transferred to the $|n\alpha\rangle$ state. The adiabaticity condition reads

$$\frac{d\alpha}{dt} \ll (\omega_L^2+\omega_S^2)^{1/2} \quad \text{or} \quad \frac{d\omega_S}{dt} \ll \frac{(\omega_L^2+\omega_S^2)^{3/2}}{\omega_L}. \tag{15}$$

The experimental implementation of this procedure was carried out by Hare *et al.* [15] to produce circular states and by Day *et al.* [16] and Mogensen *et al.* [17] for an arbitrary value of α. The radiative lifetimes of CESs were studied both experimentally and theoretically [16,17].

III. DOUBLY EXCITED COHERENT ELLIPTIC STATES

A. Formation of doubly excited coherent elliptic states

We now consider a multielectron Rydberg atom with the outer (excited) electron in a CES. Then by exciting an inner atomic electron to some higher-lying state one obtains what we label a doubly excited CES (DECES), by exciting two inner electrons one obtains a triply excited CES (TECES) and so on and so forth. In this work we shall focus on the DECESs and consider the preparation of these states in more detail. Although most of the subsequent discussion refers to the general case, we shall take the helium atom as a simple example.

In the first step, a CES is prepared by the adiabatic field switching method and absorption of an appropriate laser photon γ_1,

$$\mathrm{He}(1s^2) \overset{\vec{F},\vec{B},\gamma_1}{\rightarrow} |n_1\alpha\rangle \otimes |1s\rangle. \tag{16}$$

In the preparation of the CES, the inner electron is a spectator and remains in its $1s$ ground state orbital while the outer electron is promoted to the high-lying Rydberg state with principal quantum number n_1. Hence in Eq. (16) it is a good approximation to present the final state of the two electrons as a product of two one-electron orbitals. We discuss the effect of electron-electron correlation and the special Coulomb peculiarities pertaining also to the inner electron in the helium case in Sec. VI.

After the preparation of the outer electron in the CES, the inner electron is excited to the n_2p state with principal quantum number n_2 by the absorption of a single energetic photon γ_2 of polarization Ω,

$$|n_1\alpha\rangle \otimes |1s\rangle \overset{\gamma_2}{\rightarrow} |n_1\alpha\rangle \otimes |n_2p\rangle_\Omega. \tag{17}$$

Such a technique, known as isolated core excitation (ICE), was used extensively in experiments with multielectron Rydberg atoms, where less energetic γ_2 photons are required than in the case of the He atom, see, for instance, Ref. [18].

Depending on the polarization of the photon γ_2, different magnetic substates $|n_2pm_{\ell_2}\rangle$ of the inner electron are populated. Assuming linear polarization of the γ_2 photon, but variable direction of propagation, the final state can be presented as a coherent superposition

$$|n_2p\rangle_\Omega = -\frac{1}{\sqrt{2}}e^{-i\alpha'}\sin\beta|n_2p1\rangle + \cos\beta|n_2p0\rangle + \frac{1}{\sqrt{2}}e^{i\alpha'}\sin\beta|n_2p-1\rangle, \tag{18}$$

with parameters α' and β characterizing the polarization. Important special cases are $\beta=0$ (photon linearly polarized along z axis) and $\beta=\frac{1}{2}\pi$ (linear polarization along the x axis for $\alpha'=0$ and along the y axis for $\alpha'=\frac{1}{2}\pi$).

The DECES formed in this way is unstable against decay by autoionization,

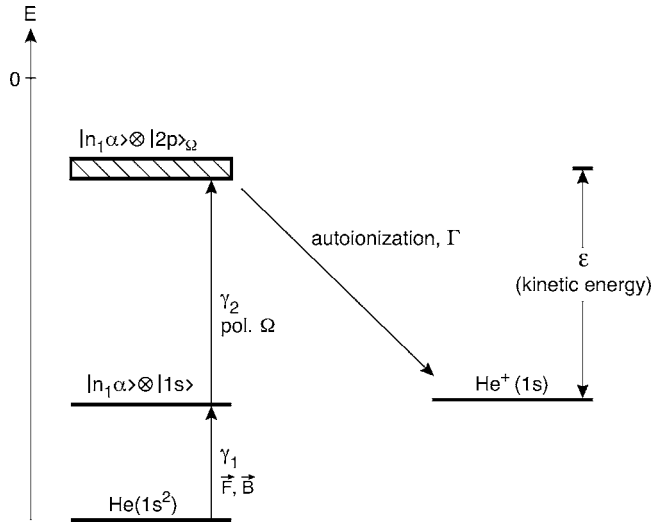

FIG. 2. Illustration of the proposed scheme for the creation of a doubly excited coherent elliptic state (DECES) in helium. First, a CES is produced by absorption of a photon γ_1 and by the adiabatic field-switching method of external $\vec{F}$ and $\vec{B}$ fields (see Sec. II). Second, the inner electron is excited by the absorption of a high-energy photon γ_2 of polarization Ω. The state obtained in this way, $|n_1\alpha\rangle \otimes |n_2p\rangle_\Omega$, is unstable to autoionization. In the figure, the inner electron is excited into the $2p$ state and hence only the autoionization decay channel to the $He^+(1s)$ is open.

$$|n_1\alpha\rangle \otimes |n_2p\rangle_\Omega \rightarrow \mathrm{He}^+(1s) + e^-(\epsilon\,\ell\,), \tag{19}$$

where ϵ is the kinetic energy of the ejected electron. In a crude approximation this latter energy is estimated by

$$\epsilon = \frac{Z^2}{2} - \frac{Z^2}{2n_2^2} - \frac{(Z-1)^2}{2n_1^2}. \tag{20}$$

In addition to the decay by autoionization, the DECES can also decay by a radiative transition of the inner electron into the ground state. Since the outer Rydberg electron remains a spectator in this process, the radiative transition width Γ_{rad} may be approximately identified with that of the $He^+(2p)$ ion. The latter is $\Gamma_{\mathrm{rad}}=2.42\times10^{-7}$ a.u., which corresponds to the lifetime $\tau=1.6$ ns [19]. Note that the radiative transitions of the Rydberg electron have much (several orders of magnitude) smaller widths (i.e., larger lifetimes) and thus can be safely neglected. The physical reason is that radiation appears due to electron acceleration, and characteristic accelerations are much lower for the Rydberg electron than for the inner one. In this study we are interested in the regime when the autoionization decay prevails over the radiative one; the preconditions are discussed below (see Fig. 2.)

B. Autoionization widths

With some modifications, we follow the theory of autoionization widths as formulated by Nikitin and Ostrovsky [7]. In that paper the widths were evaluated for the states of a two-electron atom with a definite value of the total angular momentum L and projection M,

$$\mathrm{He}^*(n_1\ell_1 n_2\ell_2 LM) \rightarrow \mathrm{He}^+(n_0\ell_0) + e^-(\epsilon\,\ell\,). \tag{21}$$

Note that L and M, as well as the total spin S, are conserved in the course of the autoionizing decay (here we neglect relativistic effects).

The states with different values of L in principle have somewhat different energies. However, in practice this splitting is very small, especially for large ℓ_1, and often not resolved in experiments. The available experimental data refer to the widths of Rydberg states with definite orbital momentum of the outer electron ℓ_1, but are not resolved over L (see, for instance, Ref. [18]). In the DECES, the outer electron does not have a definite value of quantum number ℓ_1 since the state by construction is a coherent superposition of different ℓ_1 states. The presence of many ℓ_1's implies that the quantum number L also is absent.

The widths for autoionization of initially prepared DECESs,

$$\mathrm{He}^*(n_1\alpha n_2\ell_2) \rightarrow \mathrm{He}^+(n_0\ell_0) + e^-(\epsilon\,\ell\,), \tag{22}$$

may be calculated working in an uncoupled representation of one-electron quantum numbers, or, alternatively, via a coupled LM representation. The final results are in principle equivalent, but technically each mode of derivation might have its advantages, so for completeness we consider both approaches below.

The starting point is the same in both cases. The two-electron atomic Hamiltonian is written as

$$H = H_0 + \Delta, \tag{23}$$

where H_0 is the unperturbed Hamilton operator

$$H_0 = \frac{p_1^2}{2} + \frac{p_2^2}{2} - \frac{Z_1^{\mathrm{eff}}}{r_1} - \frac{Z_2^{\mathrm{eff}}}{r_2}, \tag{24}$$

and Δ is the perturbation that leads to autoionization

$$\Delta = \frac{Z_1^{\mathrm{eff}} - Z}{r_1} + \frac{Z_2^{\mathrm{eff}} - Z}{r_2} + \frac{1}{r_{12}}, \tag{25}$$

Z is atomic nucleus charge. We introduced here the two effective charges, Z_1^{eff} and Z_2^{eff}, which are different for outer and inner electrons, to take into account the effect of screening.

The initial and final states are constructed as eigenfunctions of H_0,

$$\Psi_{\mathrm{i}}(\vec{r}_1,\vec{r}_2) = \frac{1}{\sqrt{2}}(|n_1\alpha n_2\ell_2\Omega\rangle + (-1)^S|n_2\ell_2\Omega n_1\alpha\rangle),$$

$$\Psi_{\mathrm{f}}(\vec{r}_1,\vec{r}_2) = \frac{1}{\sqrt{2}}(|\epsilon\,\ell\,m_\ell n_0\ell_0 m_0\rangle + (-1)^S|n_0\ell_0 m_0\epsilon\,\ell\,m_\ell\rangle). \tag{26}$$

Here we neglect the overlap of the inner and outer electron orbitals and present the inner electron orbital in a general form as a superposition

$$|n_2 p\rangle_\Omega = \sum_{m_2} b^\Omega_{m_{\ell,2}} |n_2 \ell_2 m_2\rangle. \tag{27}$$

The coefficients $b^\Omega_{m_2}$ are straightforwardly expressed via the parameters α' and β by comparing Eqs. (18) and (27). The general expression covers also the possibility for circular or elliptic polarization of the γ_2 photon.

1. Uncoupled one-electron angular momentum representation

The autoionization widths are given by Fermi's golden rule,

$$\Gamma_{n_1 \alpha n_2 \ell_2 \Omega \to \epsilon l m n_0 \ell_0 m_0} = 2\pi |A^\alpha_d + (-1)^S A^\alpha_e|^2, \tag{28}$$

with the matrix elements describing, respectively, direct (outer electron ejected) and exchange (inner electron ejected) autoionization (cf. Ref. [7])

$$A^\alpha_{\rm d} = \langle n_1 \alpha n_2 \ell_2 \Omega | \Delta | \epsilon l m n_0 \ell_0 m_0 \rangle = \sum_{\ell_1 m_1 m_2} c^\alpha_{\ell_1 m_1} b^\Omega_{m_2} \langle n_1 \ell_1 m_1 n_2 \ell_2 m_2 | \Delta | n_0 \ell_0 m_0 \epsilon\, \ell\, m \rangle,$$

$$A^\alpha_{\rm e} = \langle n_1 \alpha n_2 \ell_2 \Omega | \Delta | n_0 \ell_0 m_0 \epsilon\, \ell\, m \rangle = \sum_{\ell_1 m_1 m_2} c^\alpha_{\ell_1 m_1} b^\Omega_{m_2} \langle n_2 \ell_2 m_2 n_1 \ell_1 m_1 | \Delta | \epsilon l m n_0 \ell_0 m_0 \rangle. \tag{29}$$

The basic matrix elements on the right-hand side describe autoionization of atomic states with definite one-electron quantum numbers,

$$\mathrm{He}^*(n_1 \ell_1 m_1 n_2 \ell_2 m_2) \to \mathrm{He}^+(n_0 \ell_0 m_0) + e^-(\varepsilon\, \ell\, m). \tag{30}$$

To summarize the notations, $n_1 \ell_1 m_1$, $n_2 \ell_2 m_2$ denote principal, orbital and magnetic quantum numbers, respectively, for the outer and inner electron in the initial doubly excited state prior to autoionization; $n_0 \ell_0 m_0$ denote quantum numbers of the bound electron after autoionization; $\varepsilon\, \ell\, m$ are kinetic energy, orbital and magnetic quantum numbers of the electron which is ejected into the continuum. The matrix elements (29) are evaluated as

$$A_{\rm d}(n_1 \ell_1 m_1 n_2 \ell_2 m_2 | \epsilon\, \ell\, m n_0 \ell_0 m_0) \equiv \langle n_1 \ell_1 m_1 n_2 \ell_2 m_2 | \Delta | \epsilon\, \ell\, m n_0 \ell_0 m_0 \rangle$$
$$= (-1)^{\ell_1 + m_1 + \ell_2 + m_2} \sqrt{(2\ell_1+1)(2\ell_2+1)(2\ell+1)(2\ell_0+1)} \sum_{k m_k} (-1)^{k+m_k} \begin{pmatrix} \ell_1 & \ell & k \\ 0 & 0 & 0 \end{pmatrix} \begin{pmatrix} \ell_2 & \ell_0 & k \\ 0 & 0 & 0 \end{pmatrix}$$
$$\times \begin{pmatrix} \ell_1 & \ell & k \\ -m_1 & m & m_k \end{pmatrix} \begin{pmatrix} \ell_2 & \ell_0 & k \\ -m_2 & m_0 & -m_k \end{pmatrix} A^{(k)}_d (n_1 \ell_1 n_2 \ell_2 | \epsilon\, \ell\, n_0 \ell_0), \tag{31}$$

$$A_{\rm e}(n_1 \ell_1 m_1 n_2 \ell_2 m_2 | n_0 \ell_0 m_0 \epsilon\, \ell\, m) \equiv \langle n_1 \ell_1 m_1 n_2 \ell_2 m_2 | \Delta | n_0 \ell_0 m_0 \epsilon\, \ell\, m \rangle$$
$$= (-1)^{\ell_1 + m_1 + \ell_2 + m_2} \sqrt{(2\ell_1+1)(2\ell_2+1)(2\ell+1)(2\ell_0+1)} \sum_{s m_s} (-1)^{s+m_s} \begin{pmatrix} \ell_1 & \ell_0 & s \\ 0 & 0 & 0 \end{pmatrix} \begin{pmatrix} \ell_2 & \ell & s \\ 0 & 0 & 0 \end{pmatrix}$$
$$\times \begin{pmatrix} \ell_1 & \ell_0 & s \\ -m_1 & m_0 & m_s \end{pmatrix} \begin{pmatrix} \ell_2 & \ell & s \\ -m_2 & m & -m_s \end{pmatrix} A^{(s)}_e (n_1 \ell_1 n_2 \ell_2 | n_0 \ell_0 \epsilon\, \ell), \tag{32}$$

where the conventional notation for Wigner $3j$ symbols is employed, the summation indices k and s describe the multipole order in the expansion of electron-electron interaction $1/r_{12}$ that induces transition, and finally the respective partial transition amplitudes $A^{(k)}_d$ and $A^{(s)}_e$ are expressed via two-electron radial integrals

$$A^{(k)}_d (n_1 \ell_1 n_2 \ell_2 | \epsilon\, \ell\, n_0 \ell_0) = \left\langle n_1 \ell_1 n_2 \ell_2 \left| \frac{r^k_<}{r^{k+1}_>} - \delta_{k0} \frac{1}{r_1} \right| \epsilon\, \ell\, n_0 \ell_0 \right\rangle$$
$$= \int_0^\infty dr_1 r_1^2 \int_0^\infty dr_2 r_2^2 R^{(1)}_{n_1 \ell_1}(r_1) R^{(2)}_{n_2 \ell_2}(r_2) \left(\frac{r^k_<}{r^{k+1}_>} - \delta_{k0} \right) R^{(1)}_{\epsilon \ell}(r_1) R^{(2)}_{n_0 \ell_0}(r_2), \tag{33}$$

$$A^{(s)}_e (n_1 \ell_1 n_2 \ell_2 | n_0 \ell_0 \epsilon l) = \left\langle n_1 \ell_1 n_2 \ell_2 \left| \frac{r^s_<}{r^{s+1}_>} - \delta_{s0} \frac{1}{r_1} \right| n_0 \ell_0 \epsilon\, \ell \right\rangle$$
$$= \int_0^\infty dr_1 r_1^2 \int_0^\infty dr_2 r_2^2 R^{(1)}_{n_1 \ell_1}(r_1) R^{(2)}_{n_2 \ell_2}(r_2) \left(\frac{r^s_<}{r^{s+1}_>} - \delta_{s0} \right) R^{(2)}_{n_0 \ell_0}(r_1) R^{(1)}_{\epsilon \ell}(r_2). \tag{34}$$

The notations for radial wave functions $R^{(\nu_1)}_{n_1\ell_1}(r_1)$, $R^{(\nu_2)}_{n_2\ell_2}(r_2)$, $R^{(\nu_1)}_{\epsilon\ell}(r_1)$, $R^{(\nu_2)}_{n_0\ell_0}(r_2)$ are self-explanatory. The superscripts ν_i indicate effective charges Z_i^{eff}. We set $Z_1^{\text{eff}}=1$, $Z_2^{\text{eff}}=2$ [see (25)] assuming that the screening is complete. In our present treatment, the integrals (33) and (34) were evaluated numerically (for more discussion see the Appendix). For an alternative asymptotic treatment of the large angular momenta case see Ref. [7].

Although the final state magnetic quantum numbers m and m_0 are observable in principle, they are far beyond the reach of actual experiments. Therefore we consider total widths,

$$\Gamma_{n_1\alpha n_2\ell_2\Omega\to\epsilon\ell n_0\ell_0}=\sum_{mm_0}\Gamma_{n_1\alpha n_2\ell_2\Omega\to\epsilon\ell mn_0\ell_0m_0}. \tag{35}$$

After some angular momentum algebra [20] we arrive at the following general expression:

$$\begin{aligned}\Gamma_{n_1\alpha n_2\ell_2\Omega\to\epsilon\ell n_0\ell_0}=&\sum_{\ell_1m_1\ell_1'm_1'm_2m_2'}c^{\alpha}_{\ell_1m_1}c^{\alpha}_{\ell_1'm_1'}b^{\Omega}_{m_2}b^{\Omega}_{m_2'}(-1)^{\ell_1+\ell_1'}\sum_{kk'}\sum_{jm_j}(-1)^{j-m_j}(2j+1)\begin{pmatrix}\ell_1 & j & \ell_1'\\ m_1 & -m_j & -m_1'\end{pmatrix}\begin{pmatrix}\ell_2 & j & \ell_2\\ m_2 & -m_j & -m_2\end{pmatrix}\\ &\times\begin{Bmatrix}\ell_1 & j & \ell_1'\\ k' & \ell & k\end{Bmatrix}\begin{Bmatrix}\ell_2 & j & \ell_2\\ k' & \ell_0 & k\end{Bmatrix}[A_d^{(k)}(n_1\ell_1n_2\ell_2|\epsilon\,\ell\,n_0\ell_0)+(-1)^SA_e^{(k)}(n_1\ell_1n_2\ell_2|n_0\ell_0\epsilon\,\ell\,)]\\ &\times[A_d^{(k')}(n_1\ell_1'n_2\ell_2|\epsilon\,\ell\,n_0\ell_0)+(-1)^SA_e^{(k')}(n_1\ell_1'n_2\ell_2|n_0\ell_0\epsilon\,\ell\,)].\end{aligned} \tag{36}$$

While ℓ_0 can be observed experimentally since the kinetic energy ϵ depends on this quantum number, the orbital momentum ℓ of the ejected electron is not fixed in realistic experiment. Therefore the realistically observed widths of the DECESs are obtained by the expression

$$\Gamma_{n_1\alpha n_2\ell_2\Omega\to\epsilon n_0\ell_0}=\sum_{\ell}\Gamma_{n_1\alpha n_2\ell_2\Omega\to\epsilon\ell n_0\ell_0}. \tag{37}$$

In our particular case $\ell_1=1$, $\ell_0=m_0=0$ which substantially simplifies Eq. (36). The final formula looks particularly simple in the total angular momentum representation.

2. Coupled total angular momentum representation

At first we consider the autoionization process of Eq. (21) for atomic states with definite quantum numbers L and M. In this case the results of Ref. [7] apply directly. The initial and final states are constructed as

$$\Psi_i^{(LM)}(\vec{r}_1,\vec{r}_2)=\frac{1}{\sqrt{2}}(|n_1\ell_1n_2\ell_2LM\rangle+(-1)^S|n_2\ell_2n_1\ell_1LM\rangle),$$

$$\Psi_f^{(LM)}(\vec{r}_1,\vec{r}_2)=\frac{1}{\sqrt{2}}(|\epsilon\,\ell\,n_0\ell_0LM\rangle+(-1)^S|n_0\ell_0\epsilon\,\ell\,LM\rangle), \tag{38}$$

with

$$\begin{aligned}|n_1\ell_1n_2\ell_2LM\rangle&=R^{Z_1^{\text{eff}}}_{n_1\ell_1}(r_1)R^{Z_2^{\text{eff}}}_{n_2\ell_2}(r_2)\mathcal{Y}^{LM}_{\ell_1\ell_2}(\hat{\vec{r}}_1,\hat{\vec{r}}_2),\\ |\epsilon\,\ell\,n_0\ell_0LM\rangle&=R^{Z_1^{\text{eff}}}_{\epsilon\ell}(r_1)R^{Z_2^{\text{eff}}}_{n_0\ell_0}(r_2)\mathcal{Y}^{LM}_{l\ell_0}(\hat{\vec{r}}_1,\hat{\vec{r}}_2),\\ \mathcal{Y}^{LM}_{\ell_i\ell_j}(\hat{\vec{r}}_1,\hat{\vec{r}}_2)&=\sum_{m_im_j}C^{LM}_{\ell_im_i\ell_jm_j}Y_{\ell_im_i}(\hat{r}_1)Y_{\ell_jm_j}(\hat{r}_2).\end{aligned} \tag{39}$$

The autoionization widths are again given by Fermi's golden rule,

$$\Gamma^{LS}_{n_1\ell_1\ n_2\ell_2\to\epsilon ln_0\ell_0}=2\pi|A_d^L+(-1)^SA_e^L|^2, \tag{40}$$

and they do not depend on the quantum number M. The quantum numbers L and S are conserved in the autoionization process in the nonrelativistic approximation. The amplitudes of direct and exchange autoionization are, respectively,

$$\begin{aligned}A_d^L(n_1\ell_1n_2\ell_2|\epsilon\,\ell\,n_0\ell_0)&\equiv\langle n_1\ell_1n_2\ell_2LM|\Delta|\epsilon\,\ell\,n_0\ell_0LM\rangle\\ &=(-1)^L\sqrt{(2\ell_1+1)(2\ell_2+1)(2\,\ell\,+1)(2\ell_0+1)}\sum_k(-1)^k\begin{pmatrix}\ell_1 & \ell & k\\ 0 & 0 & 0\end{pmatrix}\begin{pmatrix}\ell_2 & \ell_0 & k\\ 0 & 0 & 0\end{pmatrix}\begin{Bmatrix}\ell_2 & \ell_1 & L\\ \ell & \ell_0 & k\end{Bmatrix}\\ &\times A_d^{(k)}(n_1\ell_1n_2\ell_2|\epsilon\,\ell\,n_0\ell_0),\end{aligned} \tag{41}$$

$$A_e^L(n_1\ell_1 n_2\ell_2|n_0\ell_0\epsilon l) \equiv \langle n_1\ell_1 n_2\ell_2 LM|\Delta|n_0\ell_0\epsilon\,\ell\,LM\rangle$$
$$= (-1)^{\ell+\ell_0}\sqrt{(2\ell_1+1)(2\ell_2+1)(2\,\ell\,+1)(2\ell_0+1)}\sum_s (-1)^s \begin{pmatrix} \ell_1 & \ell_0 & s \\ 0 & 0 & 0 \end{pmatrix}\begin{pmatrix} \ell_2 & \ell & s \\ 0 & 0 & 0 \end{pmatrix}\begin{Bmatrix} \ell_2 & \ell_1 & L \\ \ell_0 & \ell & s \end{Bmatrix}$$
$$\times A_e^{(s)}(n_1\ell_1 n_2\ell_2|n_0\ell_0\epsilon\,\ell\,), \tag{42}$$

where the conventional notation for $3j$ and $6j$ Wigner symbols is employed. The partial transition amplitudes are expressed via the same two-electron radial integrals as before, see Eqs. (33) and (34).

Now we turn to the widths of DECESs which have definite effective angle α, but do not possess definite total angular momentum quantum numbers L and M. In this case Fermi's golden rule gives

$$\Gamma_{n_1\alpha n_2\ell_2\to\epsilon\ell n_0\ell_0} = 2\pi\sum_{lmm_0}|A_d^\alpha + (-1)^S A_e^\alpha|^2. \tag{43}$$

We consider here realistically observable total widths summed over final state quantum numbers ℓ, m, m_0. The matrix elements of Eq. (29) are rewritten in the total angular momentum representation via the amplitudes of Eqs. (41) and (42),

$$A_d^\alpha = \langle n_1\alpha n_2\ell_2\Omega|\Delta|\epsilon\,\ell\,mn_0\ell_0 m_0\rangle = \sum_{\ell_1 m_1 m_2} c^\alpha_{\ell_1 m_1} b^\Omega_{m_2}\langle n_1\ell_1 m_1 n_2\ell_2 m_2|\Delta|\epsilon\,\ell\,mn_0\ell_0 m_0\rangle$$
$$= \sum_{\ell_1 m_1 m_2} c^\alpha_{\ell_1 m_1} b^\Omega_{m_2}\sum_{LM}(-1)^M C^{LM}_{\ell m\ell_0 m_0} C^{LM}_{\ell_1 m_1\ell_2 m_2}\langle n_1\ell_1 n_2\ell_2 LM|\Delta|\epsilon\,\ell\,n_0\ell_0 LM\rangle$$
$$= \sum_{\ell_1 m_1 m_2} c^\alpha_{\ell_1 m_1} b^\Omega_{m_2}\sum_{LM}(-1)^M C^{LM}_{\ell m\ell_0 m_0} C^{LM}_{\ell_1 m_1\ell_2 m_2} A_d^L(n_1\ell_1 n_2\ell_2|\epsilon\,\ell\,n_0\ell_0),$$

$$A_e^\alpha = \langle n_1\alpha n_2\ell_2\Omega|\Delta|n_0\ell_0 m_0\epsilon\,\ell\,m\rangle = \sum_{\ell_1 m_1 m_2} c^\alpha_{\ell_1 m_1} b^\Omega_{m_2}\sum_{LM}(-1)^M C^{LM}_{\ell m\ell_0 m_0} C^{LM}_{\ell_1 m_1\ell_2 m_2} A_e^L(n_1\ell_1 n_2\ell_2|n_0\ell_0\epsilon\,\ell\,). \tag{44}$$

Further our consideration is restricted to the simple case of interest where $\ell_0=0$ so that $L=\ell$, $M=m$. The width (43) reduces to

$$\Gamma_{n_1\alpha n_2\ell_2\to\epsilon\ell n_0\ell_0} = 2\pi\sum_{LM}\left|\sum_{\ell_1 m_1 m_2} c^\alpha_{\ell_1 m_1} b^\Omega_{m_2} C^{LM}_{\ell_1 m_1\ell_2 m_2}\right.$$
$$\times [A_d^L(n_1\ell_1 n_2\ell_2|\epsilon L n_0 0)$$
$$\left. + (-1)^S A_d^L(n_1\ell_1 n_2\ell_2|n_0 0\epsilon L)]\right|^2. \tag{45}$$

IV. RESULTS AND DISCUSSION

A. Qualitative analysis

1. Orbits approach and overlap

The objective of our study is to analyze how the autoionization widths depend on the DECES parameters, first of all the effective angle α, or the eccentricity ε that characterizes the shape of the CES of the outer electron. Another important ingredient is the state of the inner excited electron, and its orientation relative to the outer one. As mentioned in Sec. II, classical reasoning is relevant for the discussion of the outer highly excited electron.

For the classical elliptic orbit, the outer turning point r_{t2} of the radial motion always lies far from the atomic nucleus, $r_{t2}\sim n_1^2\gg 1$. The position of the inner turning point, however, depends on the shape of the ellipse through

$$r_{t1} = \frac{\ell_1^2}{1+\varepsilon} = (1-\varepsilon)n_1^2. \tag{46}$$

As $\varepsilon\to 1$, the classical outer electron penetrates the inner electron orbit ($r_1\sim r_2$) at some instants of time. This effectively enhances the average electron-electron interaction and thus induces an increase of the autoionization rate, which is *the main trend in the behavior of the ε-dependent autoionization rate* $\Gamma(\varepsilon)$. On the other hand, the penetration of the inner electron orbit by the outer electron lifts the degeneracy of Rydberg states with respect to orbital momentum, as described by ℓ-dependent quantum defects η_ℓ. The removal of degeneracy undermines the entire concept of the CES (see also the discussion in Ref. [17]). In quantum terms the penetration is characterized by an overlap of orbitals for the outer and inner electrons. The overlap depends on the relative weight of low-ℓ terms in the expansion of Eq. (12).

The condition of nonpenetration of the outer electron through the core can be written as $r_{t1}>\langle r_2\rangle$. The average distance of the inner $2p$ electron (with nucleus charge $Z=2$) is estimated as $\langle r_2\rangle=2.5$ a.u. With the help of Eq. (46), the nonpenetration condition is then expressed as

$$\varepsilon < 1 - \frac{\langle r_2\rangle}{n_1^2} = 1 - \frac{2.5}{n_1^2}. \tag{47}$$

This means that for $n_1=25$ the maximum allowed value of the eccentricity is

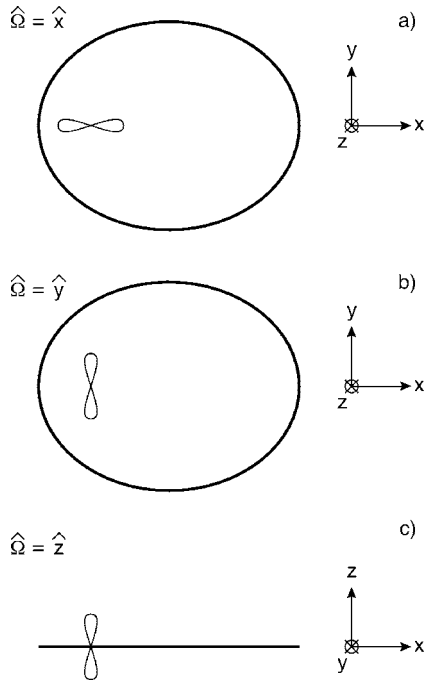

FIG. 3. Illustration of DECESs for different inner orbitals and relative orientations with respect to the CES of the outer electron. In panel (a), the $2p$ orbital is oriented along the major axis for the CES state. At perihelion there is a small distance between the two electron orbits. In panel (b), the $2p$ state is oriented along the minor axis of the ellipse. In panel (c), the ellipse is seen from the side and the $2p$ orbital is perpendicular to the plane of the ellipse.

$$\varepsilon_{25}^{\max} = 0.996, \tag{48}$$

while for $n_1=10$ the limiting value is lower, but still quite high

$$\varepsilon_{10}^{\max} = 0.975. \tag{49}$$

2. Orientation of inner electron orbital

We now consider the influence of the magnetic substate of the inner electron. We remind the reader that Eq. (13) is presuming that the electron angular momentum is quantized along the axis determined by $\vec{B}$ and perpendicular to the orbital plane of the outer electron. The same quantization axis is retained for the inner electron and we denote this axis as the z axis. We consider the excitation of the inner electron from the ground s state by a linearly polarized photon with variable direction of propagation. This allows one to populate selectively p_x, p_y or p_z substates, see Fig. 3. Looking at this figure one might expect that population of the p_x substate gives the largest autoionization width Γ_x. The relation between the widths Γ_y and Γ_z is not so obvious.

3. Electron exchange

In our treatment relativistic effects are neglected and the Hamiltonian in Eq. (23) does not depend on electron spins. The value of the total two-electron spin S is nevertheless important since it determines the symmetry of the two-electron wave function under electron permutation. This induces spin-dependent electron exchange effects which are purely quantum in their origin. It is well known that for triplet states ($S=1$) the coordinate wave function is vanishing if the coordinates of the electrons coincide, $\vec{r}_1=\vec{r}_2$. Effectively, this suppression of electronic density amounts to an extra repulsion between the electrons. As a result, one might expect suppression of autoionization of triplet states as compared to singlet ($S=0$) states. The trend should become stronger as the effective angle approaches the value $\alpha=\frac{1}{2}\pi$, i.e., $\varepsilon=1$, and the overlap of the inner and outer electron orbitals is enhanced. A convenient measure of these exchange effects is given by the ratio

$$\chi(\varepsilon) = \frac{\Gamma_{S=0}}{\Gamma_{S=1}} = \left| \frac{A_d^\alpha + A_e^\alpha}{A_d^\alpha - A_e^\alpha} \right|^2, \tag{50}$$

which is expected to be an increasing function of eccentricity ε. If the preparation of the DECES is started from the singlet ground state of an atom (as for helium or alkali-earth atoms), then, neglecting optical intercombination transitions, one obtains DECES states with $S=0$.

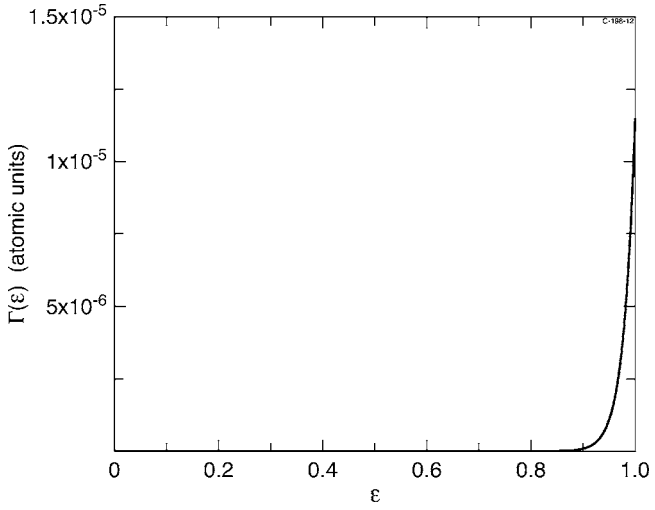

FIG. 4. Overall pattern of variation of the autoionization rate $\Gamma(\varepsilon)$ as function of eccentricity ε for $n_1=25$ and total spin $S=0$. The inner orbital is in the $2p_x$ state. The autoionization width exceeds the radiation decay width $\Gamma_{\mathrm{rad}}=2.42\times10^{-7}$ a.u. for $\varepsilon>0.92$; this regime is of primary interest in the present study.

B. Numerical results

The objective of our numerical calculations is to quantify the dependence of the autoionization widths of the DECES on the (i) eccentricity ε, (ii) orientation of the inner electron p orbit, and (iii) total electron spin S.

1. Eccentricity dependence

Figure 4 shows the dependence of the autoionization width Γ_x on the eccentricity for $n_1=25$. The inner electron is in the $2p_x$ state, where the x axis is directed along that major axis of the elliptic orbit of the Rydberg electron. The total spin is $S=0$. For eccentricities smaller than ~0.9, the auto-

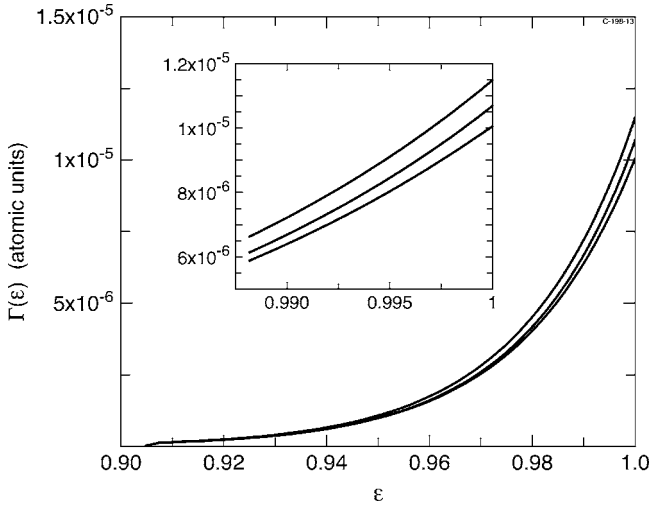

FIG. 5. Autoionization rates Γ as function of eccentricity ε in the interval $0.9<\varepsilon<1$ for $n_1=25$, $S=0$ and for different orientations of the inner electron orbital: Γ_x (upper curve), Γ_z (middle curve), Γ_y (lower curve); the subscripts x,y,z refer to the inner orbital $2p_i$, $i=x,y,z$. The inset shows a close-up for a limited range of $\varepsilon\sim 1$.

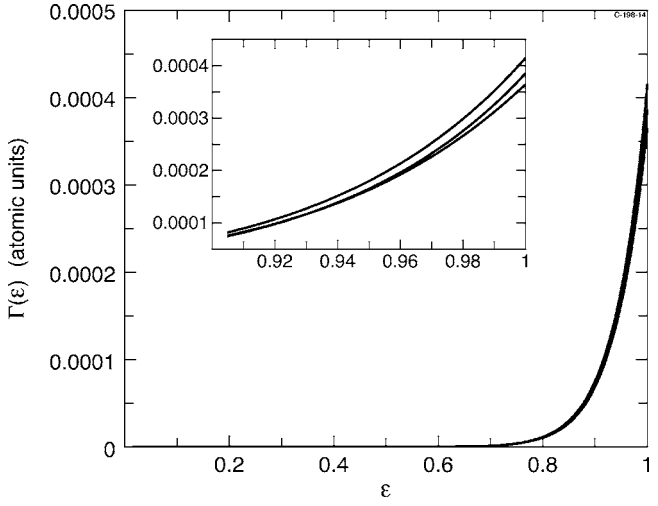

FIG. 6. As Fig. 5, but for $n_1=10$ and for different orientations of the inner electron orbital: Γ_x (upper curve), Γ_z (middle curve), Γ_y (lower curve). The inset shows a close-up for large values of ε.

ionization width is small reflecting that the two electron orbitals do not have much overlap. For larger eccentricities, the autoionization width increases rapidly with ε; it exceeds the radiation width for the inner electron, $\Gamma_x(\varepsilon)>\Gamma_{\rm rad}$ for $\varepsilon>0.92$. Under these conditions the depopulation of the DECES is governed mostly by autoionization. Since the autoionization process is of main concern in the present work, we mostly concentrate on large ε in the following. The widths in this domain are shown in more detail in Fig. 5.

The range of ε is limited from above by the applicability condition (48), $\varepsilon<\varepsilon_{25}^{\rm max}=0.996$. For $n_1=25$ the autoionization decay condition $\varepsilon>0.9$ implies that the average value of the orbital momentum of the outer electron in the CES is $\langle \ell_z\rangle \leq 10.5$, that could be compared with the range of ℓ variation for $n_1=25$: $0\leq \ell \leq 24$. The minimum distance of a classical electron from the nucleus for $n_1=25$, $r_{t1}=62.5$ a.u. for $\varepsilon=0.9$, is much larger than the extension of the inner electron orbit $\langle r_2\rangle$. The inset in Fig. 5 shows in detail this ε regime for different orientations between the plane of the ellipse and the inner $2p$ orbital. In the inset the highest, middle and lowest curves show Γ_x, Γ_z, and Γ_y, respectively, where the subscripts x,y,z refer to the inner orbital $2p_i$, $i=x,y,z$.

It is instructive to consider how the situation is changed for lower excitation of the Rydberg electron, $n_2=10$. The pattern of $\Gamma(\varepsilon)$ looks very similar (see Fig. 6), but the absolute scale of the widths is different: the maximum value $\Gamma(\varepsilon=1.0)=4.15\times 10^{-4}$ a.u. is about 40 times higher than for $n_1=25$ [$\Gamma(\varepsilon=1.0)=1.15\times 10^{-5}$ a.u.]. Due to this the condition $\Gamma_x(\varepsilon)>\Gamma_{\rm rad}$ is satisfied already for $\varepsilon>0.63$. This provides a broad window for application of the present theory, although the upper-side applicability condition (49) is somewhat more restrictive than for $n_1=25$.

2. Orientation of 2p orbitals

Figure 5 displays $\Gamma(\varepsilon)$ curves for different orientations of the p-orbital of the inner electron (see Fig. 3). The overall patterns of Γ_x, Γ_y, and Γ_z are the same for all the curves. Some difference in absolute values appears as ε tends to unity, i.e., when the orbits of the Rydberg electron and the inner electron approach each other at some intervals of time. The ordering obtained from the calculations reads

$$\Gamma_x>\Gamma_z>\Gamma_y. \tag{51}$$

As indicated above, the fact that the width Γ_x is the largest one is expected from qualitative reasoning while the relative ordering of Γ_x and Γ_y is less obvious. The situation for $n_1=10$ is very similar, see Fig. 6.

3. Role of exchange

In Fig. 7 we investigate the influence of the total spin of the two electrons on the autoionization process. The figure illustrates, as expected from qualitative reasoning, that sin-

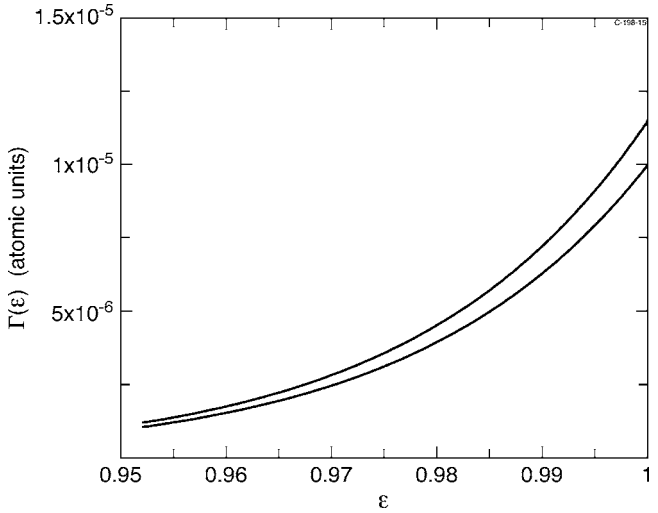

FIG. 7. Autoionization width $\Gamma(\varepsilon)$ for the singlet (upper curve) and triplet (lower curve) states; $n_1=25$. The inner electron is in the $2p_x$ orbital.

glet states have larger autoionization widths than triplet states, $\Gamma_{S=0} > \Gamma_{S=1}$. This means that direct terms dominate over exchange terms. The relative contribution to autoionization via the exchange process is characterized by the χ parameter of Eq. (50). It is maximal for the largest $\varepsilon = 1$. For $\varepsilon = 1$ the parameter χ takes the value

$$\chi(\varepsilon = 1) = 1.15, \tag{52}$$

obtained numerically for $n_1 = 25$. Interestingly, the calculations for $n_1 = 10$ give practically the same result. The value $\chi(\varepsilon = 0)$ is very close to 1.

Although the increase of the function $\chi(\varepsilon)$ with ε is well expected, its actual stepwise behavior comes as a surprise, see Fig. 8. For the $n_1 = 25$ case (full curve), the steep raise starts at $\varepsilon = 0.5$ whereafter the value of the $\chi(\varepsilon)$ function is close to its maximum value, 1.15. Therefore $\chi(\varepsilon = 1)$ is a convenient characteristic parameter, although the theory becomes inapplicable in the limit $\varepsilon \to 1$, as discussed above. The details of the $\chi(\varepsilon)$ behavior depend on the value of n_1, thus for $n_1 = 10$ (dashed curve) the steep rise starts at $\varepsilon \sim 0.1$. In addition, a shallow minimum appears around $\varepsilon = 0.45$; this feature is difficult to interpret qualitatively.

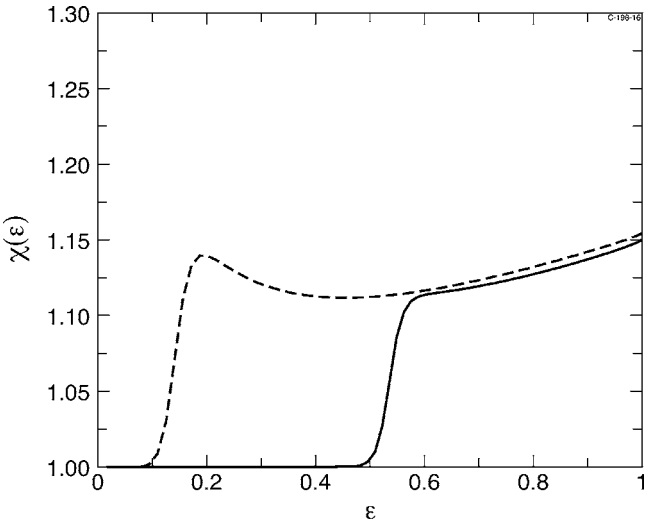

FIG. 8. Exchange parameter $\chi(\varepsilon)$, see discussion in text. The inner electron is in the $2p_x$ orbital. The full curve shows the result for $n_1 = 25$, the dashed curve shows the result for $n_1 = 10$.

V. REMARKS ON COHERENCE AND ELECTRON-ELECTRON CORRELATION

A. Coherence

We start with a one-electron system. Equation (12) presents the CES $|n\alpha\rangle$ as a superposition of spherical $|n\ell m_\ell\rangle$ states with different orbital ℓ and magnetic m_ℓ quantum numbers. This is a coherent superposition which is directly manifested by the fact that if the superposition coefficients $c^{\alpha}_{n\ell m}$ are multiplied by different phase factors $\exp(i\phi_{n\ell m})$, then the resulting wave function will change, and for instance, the electron density will become different. However, this does not exclude that some physical observables could prove to be insensitive to the introduction of such a state-specific phase change. This was, e.g., shown to be the case for the total radiative decay from CESs [17,21]: For any CES, the radiative decay width is expressed via widths for the spherical states, i.e., via modulus squared transition matrix elements; the relative phases of the matrix elements do not play a role. This property may be called stability against dephasing.

Dephasing transformations occur naturally as a consequence of propagation in time. Indeed, the CES presents a coherent superposition of spherical $|n\ell m_\ell\rangle$ states. If the external fields are switched off and the Rydberg atom has some non-Coulomb core, then each $|n\ell m_\ell\rangle$ state has somewhat different energy characterized by the ℓ-dependent quantum defects η_ℓ. Due to these differences in energy, different $|n\ell m_\ell\rangle$ components in the superposition gain different phase factors $\exp[i(\eta_\ell/n^3)t]$ and as time t passes this results in dephasing. The stability against dephasing is a favorable circumstance in the sense that it simplifies the experimental observation of a CES. On the other hand, dephasing could be considered as a physically interesting effect for study.

It follows from Eq. (45) that the autoionization width of DECESs depends on phases of the coefficients $c^{\alpha}_{n\ell m}$, i.e., it is unstable against dephasing. As in the case of CESs, the time-propagation-induced dephasing depends on the energy level structure. A description of the details of this structure requires account for electron-electron correlation.

B. Electron-electron correlations

The present calculations do not take into account electron-electron correlations as seen from the factorized representation of the two-electron wave function in Eq. (17). Generally, electron-electron correlations are known to be essential in the description of autoionizing doubly excited states. The correlation becomes especially strong when the inner electron moves in a pure Coulomb field, as is the case for the He atom. Specifics of He are briefly discussed below. Although this atom is very important from the fundamental point of view one should bear in mind that all other atoms have a non-Coulombic core. The present study is in fact oriented on this more generic case, although in the calculations we used wave functions and orbital energies for the simplest case, the He atom. Thus we investigated the principal properties of DECESs in case of weak correlations; the assessment of correlation effects remains a subject for future studies.

The specifics of He stem from the fact that the inner electron states are, in a good approximation, degenerate in the orbital number ℓ_2. This means that Stark states which possess an electric dipole moment may be formed in the course of the interaction and the outer electron would then move in a superposition of Coulomb and dipole potentials. Moreover, the dipole moment of the inner electron depends on the state of the outer electron. This situation is quantum mechanically described by correlated (i.e., nonfactorized entangled) two-electron wave functions known as *dynamic dipole states* or *planetary atom states*. The problem of planetary states has been discussed extensively in the literature. The theory for two-electron atoms was developed in Refs. [22,23] and reviewed in Ref. [3]. Up to now experiments were carried out for multielectron (alkaline earth) atoms [24,25]. More recent

experiments with pulsed laser excitation (e.g., half-cycle pulses) required development of theory in the time domain [26].

The second step in the formation of DECES is accompanied by a shake-up of the outer electron due to a sudden change of its interaction with the core. This change in the interaction, as well as the correlation-induced structure of the energy levels, introduce dephasing transitions and require detailed analysis with account for the bandwidth of the γ_2 photons. Such analysis is beyond the scope of the present paper that aimed to introduce DECES as a subject of future studies.

VI. CONCLUSION AND OUTLOOK

The main objectives of the present work were to introduce doubly excited coherent elliptic states (DECESs) as an interesting object to study and to explore the major trends in the autoionization of DECESs. The DECESs present part of a vast Rydberg state realm where quantum and classical features meet and interplay. The CES ingredient of the DECES is of interest since it allows a continuous transition between the limiting cases of circular and Stark states. And due to the adiabatic field-switching technique the CESs are relatively easy to produce experimentally. In this work, we quantitatively demonstrated the dependence of the autoionization widths on (i) CES eccentricity, (ii) degree of the Rydberg state excitation, (iii) orientation of the inner electron p orbital, and (iv) electron exchange effects. The competition between radiative and autoionization decay of DECES was assessed. The existence of a rather broad parameter range where the DECES decay is governed by autoionization was demonstrated.

As a generic case we referred to the helium atom with inner electron excitation to the lowest p orbital. This latter step requires a UV source of photons. We also note that the He^+ ion has the smallest possible size, which is favorable for the creation of DECES. As the size of the core increases, the upper bound of the value of the eccentricity ε becomes more restrictive. An obvious extension of the present study is to consider excitation of the inner electron to higher p states. Apart from an increase in the size of the core, a new phenomenon emerges: the possibility of autoionizing decay with population of excited states of the residual ion. The autoionization process would then be characterized by partial autoionization widths to the different ionic target states. These widths could also be evaluated within the present approach. With more open decay channels available, the propensity rule reads that autoionization with ejection of a low energy electron is preferable.

The transition to multielectron atoms implies further increase of the core size. The core energy levels have richer structure, so that excitations of different terms within the same multiplet might be considered. This would require lower photon energies than in the helium case. Furthermore, the larger core size imposes more stringent restrictions on the existence of CES with respect to the eccentricity. The core polarization effects and Rydberg series interaction are to be taken into account in a quantitative analysis (the large angular momenta case was considered by Poirier [27,28]).

Finally, we note that the concept of DECESs could be extended to multiply excited coherent elliptic states. For instance, the coherent control of the outer Rydberg electron could be expected to shed new light on the autoionization mechanisms in triply excited states [4].

ACKNOWLEDGMENTS

The authors thank Erik Horsdal-Pedersen for useful discussions. The present work was supported by the Nordic Research Board NordForsk. One of the authors (L.B.M.) was supported by the Danish Natural Science Research Council (Grant No. 21-03-0163) and the Danish Research Agency (Grant. No. 2117-05-0081).

APPENDIX: INTEGRALS

The radial integrals (33) and (34) containing $r_<$, $r_>$ symbols are presented in more detail as

$$
\begin{aligned}
A_d^{(k)} &= \left\langle n_1\ell_1 n_2\ell_2 \left| \frac{r_<^k}{r_>^{k+1}} - \delta_{k0}\frac{1}{r_1} \right| \epsilon\,\ell\, n_0\ell_0 \right\rangle \\
&= \int_0^\infty dr_1 r_1^{1-k} R^{(1)}_{n_1\ell_1}(r_1) R^{(1)}_{\epsilon l}(r_1) \int_0^{r_1} dr_2 r_2^{k+2} R^{(2)}_{n_2\ell_2}(r_2) R^{(2)}_{n_0\ell_0}(r_2) \\
&\quad + \int_0^\infty dr_2 r_2^{1-k} R^{(2)}_{n_2\ell_2}(r_2) R^{(2)}_{n_0\ell_0}(r_2) \int_0^{r_2} dr_1 r_1^{k+2} R^{(1)}_{n_1\ell_1}(r_1) \\
&\quad \times R^{(1)}_{\epsilon\ell}(r_1) - \delta_{k0}\Bigg(\int_0^\infty dr_1 r_1 R^{(1)}_{n_1\ell_1}(r_1) R^{(1)}_{\epsilon\ell}(r_1) \int_0^{r_1} dr_2 r_2^2 \\
&\quad \times R^{(2)}_{n_2\ell_2}(r_2) R^{(2)}_{n_0\ell_0}(r_2) + \int_0^\infty dr_2 r_2^2 R^{(2)}_{n_2\ell_2}(r_2) R^{(2)}_{n_0\ell_0}(r_2) \\
&\quad \times \int_0^{r_2} dr_1 r_1 R^{(1)}_{n_1\ell_1}(r_1) R^{(1)}_{\epsilon\ell}(r_1) \Bigg),
\end{aligned} \tag{A1}
$$

$$
\begin{aligned}
A_e^{(s)} &= \left\langle n_1\ell_1 n_2\ell_2 \left| \frac{r_<^s}{r_>^{s+1}} - \delta_{s0}\frac{1}{r_1} \right| n_0\ell_0\epsilon l \right\rangle \\
&= \int_0^\infty dr_1 r_1^{1-s} R^{(1)}_{n_1\ell_1}(r_1) R^{(2)}_{n_0\ell_0}(r_1) \int_0^{r_1} dr_2 r_2^{s+2} R^{(2)}_{n_2\ell_2}(r_2) R^{(1)}_{\epsilon\ell}(r_2) \\
&\quad + \int_0^\infty dr_2 r_2^{1-s} R^{(2)}_{n_2\ell_2}(r_2) R^{(1)}_{\epsilon\ell}(r_2) \int_0^{r_2} dr_1 r_1^{s+2} R^{(1)}_{n_1\ell_1}(r_1) \\
&\quad \times R^{(2)}_{n_0\ell_0}(r_1) - \delta_{s0}\Bigg(\int_0^\infty dr_1 r_1 R^{(1)}_{n_1\ell_1}(r_1) R^{(2)}_{n_0\ell_0}(r_1) \\
&\quad \times \int_0^{r_1} dr_2 r_2^2 R^{(2)}_{n_2\ell_2}(r_2) R^{(1)}_{\epsilon\ell}(r_2) + \int_0^\infty dr_2 r_2^2 R^{(2)}_{n_2\ell_2}(r_2) \\
&\quad \times R^{(1)}_{\epsilon\ell}(r_2) \int_0^{r_2} dr_1 r_1 R^{(1)}_{n_1\ell_1}(r_1) R^{(2)}_{n_0\ell_0}(r_1) \Bigg).
\end{aligned} \tag{A2}
$$

For the doubly excited states with $n_1 \gg n_0$ the exchange integral (A2) is governed by the overlap of radial wave unctions $R^{(1)}_{n_1\ell_1}(r)$ and $R^{(2)}_{n_0\ell_0}(r)$, which is small.

For maximal $\ell_1 = n_1 - 1$ the function $R^{(1)}_{n_1(n_1-1)}(r)$ is localized mostly in the interval $n_1^2 - n_1 < r < n_1^2 + n_1$ while the function $R^{(2)}_{n_0\ell_0}(r)$ is localized at small $r \sim n_2 \sim 1$. Therefore the overlap is small. As ℓ decreases, the localization domain extends to smaller ℓ and the overlap with $R^{(2)}_{n_0\ell_0}(r)$ orbital is enhanced. The weight of large orbital momenta in the CES increases as ε tends to zero.

[1] R. P. Madden and K. Codling, Phys. Rev. Lett. **10**, 516 (1963).
[2] U. Fano, Phys. Rev. **124**, 1866 (1961).
[3] G. Tanner, K. Richter, and J. M. Rost, Rev. Mod. Phys. **72**, 497 (2000).
[4] L. B. Madsen, J. Phys. B **36**, R223 (2003).
[5] U. Fano and J. W. Cooper, Phys. Rev. **137**, A1364 (1965).
[6] L. B. Madsen, J. Phys. B **34**, 2137 (2001).
[7] S. I. Nikitin and V. N. Ostrovsky, J. Phys. B **13**, 1961 (1980).
[8] F. Roussel, M. Chéret, L. Chen, T. Bolzinger, G. Spiess, J. Hare, and M. Gross, Phys. Rev. Lett. **65**, 3112 (1990); L. Chen, M. Chéret, M. Poirier, F. Roussel, T. Bolzinger, and G. Spiess, J. Phys. II **2**, 701 (1992).
[9] M. Born, *The Mechanics of the Atom* (G. Bell and Sons, London, 1927), reprinted by Ungar, New York, 1967.
[10] Yu. N. Demkov, B. S. Monozon, and V. N. Ostrovsky, Zh. Eksp. Teor. Fiz. **57**, 1431 (1969) [Sov. Phys. JETP **30**, 775 (1970)].
[11] A. Bommier, D. Delande, and J. C. Gay, in *Atoms in Strong Fields*, edited by C. A. Nicolaides *et al.* (Plenum, New York, 1990).
[12] R. J. Glauber, Phys. Rev. **130**, 2529 (1963).
[13] D. Delande and J. C. Gay, Europhys. Lett. **5**, 303 (1988).
[14] J. C. Gay, D. Delande, and A. Bommier, Phys. Rev. A **39**, 6587 (1989).
[15] J. Hare, M. Gross, and P. Goy, Phys. Rev. Lett. **61**, 1938 (1988).
[16] J. C. Day, T. Ehrenreich, S. B. Hansen, E. Horsdal-Pedersen, K. S. Mogensen, and K. Taulbjerg, Phys. Rev. Lett. **72**, 1612 (1994).
[17] K. S. Mogensen, J. C. Day, T. Ehrenreich, E. H. Pedersen, and K. Taulbjerg, Phys. Rev. A **51**, 4038 (1995).
[18] W. E. Cooke, T. F. Gallagher, S. A. Edelstein, and R. M. Hill, Phys. Rev. Lett. **40**, 178 (1978).
[19] B. H. Bransden and C. J. Joachain, *Physics of Atoms and Molecules* (Longman Scientific and Technical, New York, 1995).
[20] D. A. Varshalovich, A. N. Moskalev, and V. K. Khersonsky, *Kvantovaya Teoriya Uglovogo Momenta* (Nauka, Leningrad, 1975) [English translation: *Quantum Theory of Angular Momentum* (World Scientific, Singapore, 1988)].
[21] M. Mijatovic, E. A. Solov'ev, and K. Taulbjerg, J. Phys. B **34**, 1897 (2001).
[22] S. I. Nikitin and V. N. Ostrovsky, J. Phys. B **11**, 1681 (1978); P. A. Braun, V. N. Ostrovsky, and N. V. Prudov, Phys. Rev. A **42**, 6537 (1990); V. N. Ostrovsky, Phys. Rev. A **46**, R5309 (1992); V. N. Ostrovsky, J. Phys. B **26**, 1163 (1993); V. N. Ostrovsky and N. V. Prudov, *ibid.* **26**, L263 (1993); Phys. Rev. A **51**, 1936 (1995); J. Phys. B **28**, 4435 (1995); **30**, 151 (1997); N. V. Prudov and V. N. Ostrovsky, Phys. Rev. Lett. **81**, 285 (1998).
[23] K. Richter and D. Wintgen, Phys. Rev. Lett. **65**, 1965 (1990); J. Phys. B **24**, L565 (1992); K. Richter, J. M. Rost, R. Thürwächter, J. S. Briggs, D. Wintgen, and E. A. Solov'ev, Phys. Rev. Lett. **66**, 149 (1991); K. Richter, J. S. Briggs, D. Wintgen, and E. A. Solov'ev, J. Phys. B **25**, 3929 (1992).
[24] P. Camus, T. F. Gallagher, J.-M. Lecomte, P. Pillet, L. Pruvost, and J. Boulmer, Phys. Rev. Lett. **62**, 2365 (1989); P. Camus, J.-M. Lecomte, C. R. Mahon, P. Pillet, and Pruvost, J. Phys. II **2**, 715 (1992); P. Camus, S. Cohen, L. Pruvost, and A. Bolovinos, Phys. Rev. A **48**, R9 (1993).
[25] U. Eichmann, V. Lange, and W. Sandner, Phys. Rev. Lett. **64**, 274 (1990); **68**, 21 (1992); K.-D. Heber, M. Seng, M. Halka, U. Eichmann, and W. Sandner, Phys. Rev. A **56**, 1255 (1997); C. Rosen, M. Dörr, U. Eichmann, and W. Sandner, Phys. Rev. Lett. **83**, 4514 (1999).
[26] S. N. Pisharody and R. R. Jones, Phys. Rev. A **65**, 033418 (2002); J. G. Zeibel, S. N. Pisharody, and R. R. Jones, *ibid.* **67**, 013409 (2003); S. N. Pisharody and R. R. Jones, Phys. Rev. Lett. **91**, 203002 (2003); Science **303**, 813 (2004).
[27] M. Poirier, Phys. Rev. A **38**, 3484 (1988).
[28] M. Poirier, Phys. Rev. A **63**, 052513 (2001).